

# A Helium Cluster Beam Source for Cluster Isolated Chemical Reaction Studies

M.A. Gaveau and P.R. Fournier

Laboratoire Francis Perrin, CNRS URA 2453, DSM/DRECAM/SPAM,  
C.E.A. Saclay, F-91191 Gif-sur-Yvette Cedex, France  
marc-andre.gaveau@cea.fr

**Abstract.** In our laboratory, we have developed the CICR technique (Cluster Isolated Chemical Reactions) to study elementary chemical processes at the surface of large van der Waals clusters, in order to analyze the effect of the “environment medium” on reaction dynamics. In the last years, we have worked on clusters only generated from room temperature like  $\text{Ar}_n$  and  $(\text{N}_2)_n$ , or liquid nitrogen temperature like  $(\text{CH}_4)_n$  and  $\text{Ne}_n$ . More recently, we decided to extend our studies to superfluid helium clusters with a very low temperature (0.4 K) and a very weak interaction with the trapped reactants. For this purpose, we had to design a cooled jet source to be able to achieve a reservoir temperature  $T_0$  as low as 10 K, in order to produce in our experiment a continuous beam of sufficiently large helium clusters. This source uses a two-stage cold head which had to be fitted to the existing vacuum chambers, and this was not a trivial problem.

The recent results show the presence of large helium clusters in the He time-of-flight distributions, for stagnation pressures  $P_0$  up to 72 bars with  $T_0 = 13.5$  K in this case. The lower stagnation temperatures  $T_0$ , ranging between 9.5 and 11.5 K, are obtained for stagnation pressures between 6 and 25 bars. At 6 bars, the condensation is not complete, and the time-of-flight distribution displays two separated peaks for monomers and clusters.

At higher stagnation pressure  $P_0 = 20$  bars ( $T_0 = 11$  K), the cluster size is large enough to capture calcium atoms by the pick-up technique, so that we can obtain laser induced fluorescence signal by an excitation wavelength around 380 nm. It is also possible to perform successive pick-ups of two reactants (for example Ca and  $\text{NO}_2$ ) to observe the fluorescence from their chemical reaction on helium clusters.

**Keywords:** helium cluster; superfluidity ; supersonic free jet; chemical reactivity; pick-up; laser induced fluorescence; calcium;  $\text{NO}_2$

**PACS:** 39.10.+j 36.40.-c 82.33.Hk

## INTRODUCTION

During the last few years, we have developed in our laboratory the CICR technique (Cluster Isolated Chemical Reactions) [1, 2, 3] to investigate the effect of a reaction medium on the reaction dynamics in order to have an approach to the heterogeneous chemistry at a microscopic level. An ideal experiment would consist in isolating a single elementary reactive process in a well defined environment, i.e. a reaction medium whose size, structure, temperature, and interaction with the reactants, would be known. For this purpose we have chosen to take the cluster as the reaction medium and use it as a true micro chemical reactor in the CICR method.

All over this period, we have worked on spectroscopy and dynamics of alkaline earth atoms (Ba [4, 5] and Ca [6]) and dimers [7] on different types of large van der Waals clusters. We have also studied the Cluster Isolated Chemical Reactivity of these metals. In particular, we have studied chemiluminescent reactions of monomers like Ba with  $\text{N}_2\text{O}$  [8, 9, 10] or multimers such as  $\text{Ba}_2$  with  $\text{CO}_2$  or  $\text{Ba}_3$  with  $\text{SF}_6$  [11].

We also worked on photoinduced reactions in endothermic systems like  $\text{Ca} + \text{Br}$  deposited on argon and neon clusters [12] and exothermic systems like  $\text{Ca} + \text{CH}_3\text{F}$  deposited on argon clusters [13].

At the same time, there has been a considerable development in the field of helium clusters following the pioneering work of E.W. Becker in the sixties, and J. Gspann in the seventies and early eighties (see for example Ref. [14] and references therein). Afterwards, a lot of groups (G. Scoles, J.P. Toennies, R.E. Miller, etc ...) worked on helium clusters, pure or seeded by one or more atoms and molecules (see in particular the reviews [15, 16]). They used the very specific properties of this medium (superfluidity, very low temperature, and weak interaction) to perform spectroscopic experiments in the visible [17] or in the IR [18, 19] ranges, or reactivity experiments [20].

Previously, in our laboratory, we have only used clusters generated from a source at room temperature or cooled with liquid nitrogen. It was obviously of interest to extend the CICR experiments to helium clusters. Thus, we have modified our Campargue beam source (see review article [21] and refs. therein) and use it as a helium cluster beam source: this paper presents its characteristics and the first results.

## EXPERIMENT

### CICR Principle and Experimental Setup

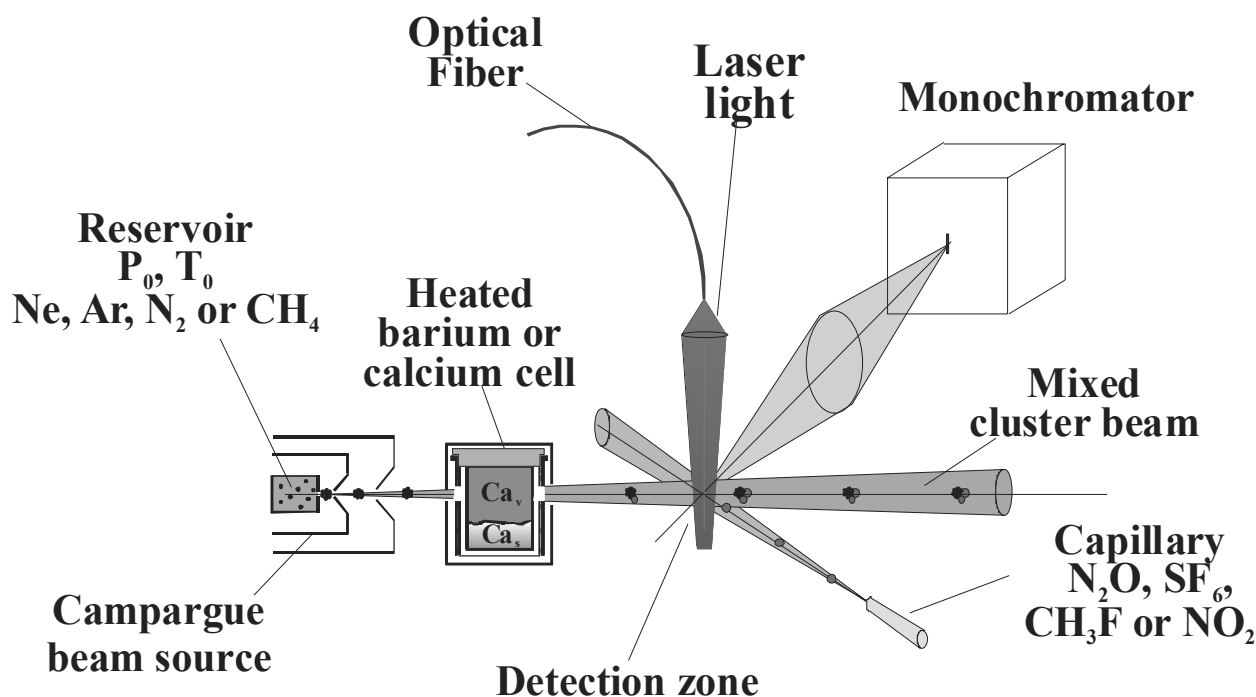


FIGURE 1. Experimental Setup

The experimental setup is shown schematically in Figure 1.

Clusters are grown by condensation in a continuous supersonic free jet of the Campargue type [21], with a reservoir at pressure  $P_0$  ( $<50$  bars) and at temperature  $T_0$  ( $<300$  K). After extraction from the jet by a skimmer of 1 mm diameter, the beam passes through a differentially pumped chamber prior to entering the main chamber through a 3 mm collimator.

Reactants are deposited on clusters by collisional capture, i.e. the pick-up technique [22]: for example, in the  $Ca + CH_3F$  experiment, the Ar cluster beam passes through a heated cell containing a low pressure of calcium vapor ( $10^{-4}$  to  $10^{-3}$  mbar), where clusters trap eventually one or several calcium atoms. Then, 17 mm downstream, the cluster beam crosses an effusive beam of  $CH_3F$  molecules which are also captured by clusters.

In the pick-up technique, the reactants are captured at the surface of the cluster and we have shown that calcium remains at the surface in the case of argon and neon clusters [6]. Then, the reactants migrate and explore the surface of the cluster on a nanosecond timescale, to finally collide and eventually react.

The second pick-up zone can also be illuminated by the light from a single frequency tunable CW laser beam to photoinduce a chemical reaction as in the  $Ca + CH_3F$  system or perform laser induced fluorescence diagnostics. The light from these lasers (dye laser or titanium-sapphire laser eventually doubled by an extra cavity doubler) is transported into the reaction zone by an optical fiber (0.6 mm core diameter). The output of the fiber is refocused into a slightly converging beam crossing the cluster beam at right angle.

This second pick-up region, which is also the observation zone, is imaged onto the entrance slit of a scanning grating monochromator by means of an optical collection device. The luminescence signal is detected by a cooled photomultiplier tube (RCA 31034). The photon counting technique is used for detection. After fast amplification and discrimination, the signal is accumulated using multiscaler cards implemented in a microcomputer.

The reaction signal is analyzed either through the chemiluminescence of electronically excited products or the Laser Induced Fluorescence (LIF) of products in their ground state, or even the ionic signal of the products by mass spectrometers that are housed in the last chamber of the setup. It is also possible to use LIF or mass spectrometry to detect the reactants and even measure their abundances on the cluster.

A main advantage of the CICR method is that it is quantitative: it is possible to control the average number of reactants trapped per cluster by controlling the pressure of the pick-up gas. For example, if the temperature of the pick-up cell is varied, the vapor pressure of the metal changes in the same way as the average number of reactants captured by the cluster. Measuring the variation of the reaction signal as a function of the number of reactants allows us to deduce the order of the reaction, i.e. the number of reactants involved in the reaction process [2].

So far, we have only used clusters that could be generated from room temperature, as for argon or nitrogen, or from the source cooled by liquid nitrogen, as for methane or neon. The average cluster sizes  $\langle N \rangle$  obtained for the various gases as a function of the initial conditions, are summarized in Table 1.

**TABLE 1. Average cluster size  $\langle N \rangle$  as a function of initial conditions.**

Gas	$P_0$ (bars)	$T_0$ (K)	Nozzle type Diameter (mm)	Average size $\langle N \rangle$
Argon	20	290	Sonic 0.2	2000
Nitrogen	28	290	Conical 0.08	3000
Methane	20	226	Sonic 0.2	1200
Neon	30	83	Sonic 0.1	7000

## THE HELIUM CLUSTER BEAM SOURCE

In order to produce helium clusters with  $\langle N \rangle$  large enough to pick-up several reactants for CICR experiment at very low temperature, we had to modify considerably our molecular beam source. As it can be observed in the phase diagram of helium [23], the liquid-vapor line has a very small extension with a critical point at a very low temperature  $T_c = 5.2$  K and pressure  $P_c = 2.3$  bars. The formation of helium clusters in the free jet expansion needs a very low temperature  $T_0$  in the reservoir and a sufficiently high stagnation pressure  $P_0$ . So, from the experience of many different groups already working with helium clusters [14, 15, 16], we know that we must obtain a source temperature  $T_0$  of about 10 K with a stagnation pressure  $P_0$  at least of 20 bars, while maintaining a background pressure lower than  $10^{-3}$  mbars in the expansion chamber. Furthermore, the nozzle of 5  $\mu$ m diameter must keep a very stable position as the stagnation temperature  $T_0$  decreases from room temperature to 10 K in order to maintain a high flux in the cluster beam.

### Design of the cooled molecular beam source: technical problems and solutions

We decided to cool the beam source not by means of liquid helium, but by using a more convenient and cheaper technique. So, we based the design of the cooled jet source on a two-stage cryo-cooler SUMITOMO RDK 408 which has a refrigeration capacity of 35 W at 40 K on the first stage, and 1 W at 4.2 K on the second stage.

We had to fit the cooled source to the existing two interlinked chambers (see Figure 2), both for practical reasons and also to keep the advantages of the available Campargue beam source. However, the adaptation of the source presented several difficulties:

- The diameter of the source has to be limited to 130 mm,
- The length of the source inside the expansion chamber is about 1 m,
- The axial alignment of the source is achieved using a guiding cylinder connected to the expansion chamber and mechanically aligned with the skimmer and the collimator,
- The pumping speed of the expansion chamber is limited by the relatively small diameter (150 mm) of the pumping connexion.

So the modified source is composed of parts listed as follows (Figure 3):

- The two-stage cold head,

- An external cylinder of Duraluminium at room temperature, allowing to drive axially the whole source in the guiding cylinder,
- A thermal insulating nose fixed at the end of this cylinder,
- An external copper shield maintained by the insulating nose and connected to the first stage of the cold head at 30 K,
- The internal copper rod (diameter 30 mm, length 696 mm), that supports the nozzle. This colder part is attached to the second stage of the cold head ( $\sim 5\text{K}$ ) and axially aligned by the insulating nose.

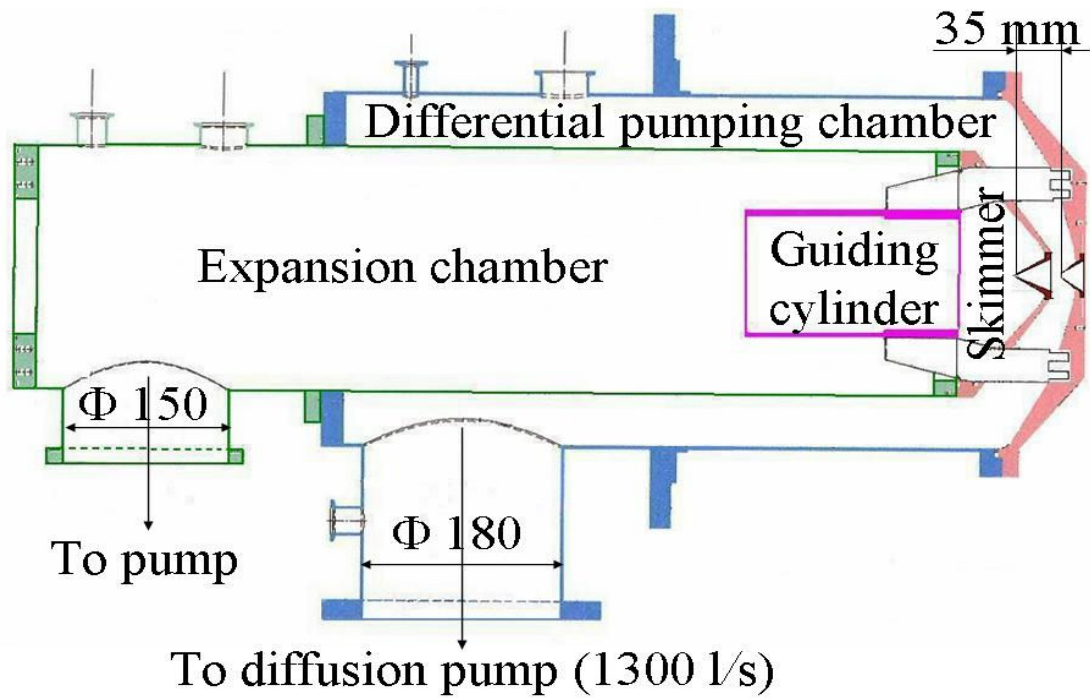


FIGURE 2. The available source chambers (Campargue beam)

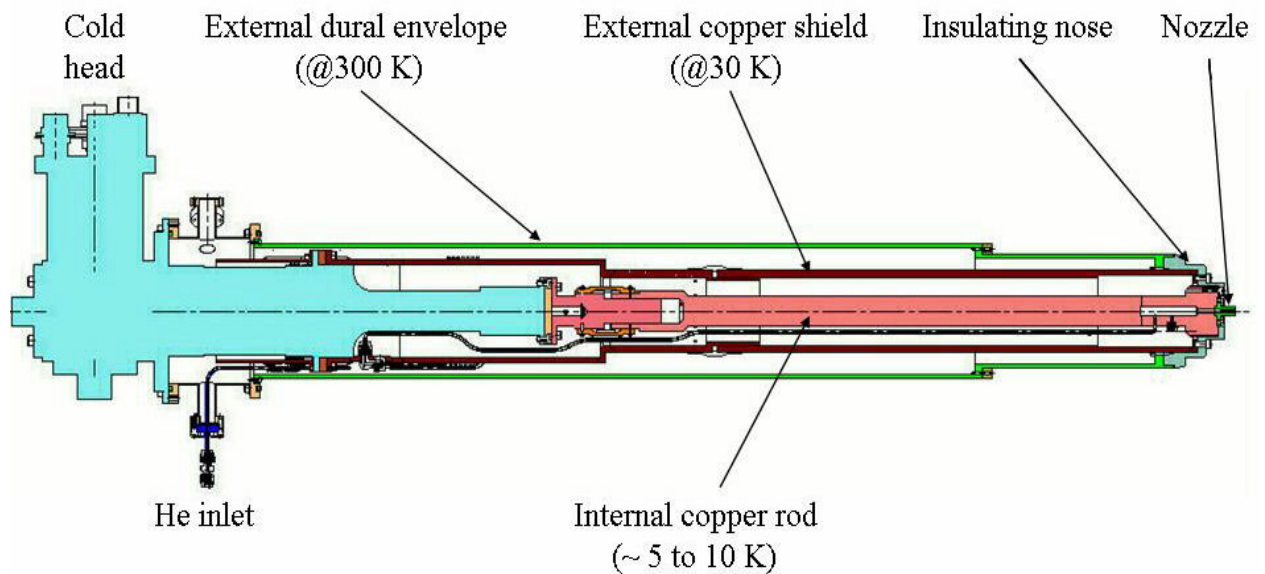


FIGURE 3. The cooled source for helium cluster beam production

The external cylinder at room temperature and the insulating nose keep constant the length of the source and fix the position of the nozzle. So the external copper shield and the internal part are both made of two sliding pieces linked together by copper meshes in order to balance the thermal contraction due to the extreme cooling while keeping an efficient thermal conductivity.

The cooled internal walls of the beam source are also covered with aluminized Mylar foils used as radiation shields. The temperature is monitored by 3 silicon diodes and one platinum resistor sensor. The temperature of the nozzle can be controlled through resistive heating of the central part under proportional integral differential control (LakeShore Model 321 S). The cold source length is slightly greater than 1 meter. The expansion chamber is pumped by a VARIAN turbomolecular pump, having a relatively low pumping speed (1000 l/s) as compared with those commonly used in such sources [16]. This pump has a large compression factor for helium, and can keep a good pumping speed at relatively high pressure. It can also be helped for high stagnation pressure ( $P_0 > 20$  bars) by the available Roots pumps (2000 m<sup>3</sup>/h) of the Campargue beam source pumping in parallel the expansion chamber.

## THE HELIUM CLUSTER BEAM SOURCE: EXPERIMENTAL RESULTS AND CHARACTERISTICS

When a temperature sufficiently low (below 20 K) is reached in the source, we can check the presence of clusters in the beam. There are at least five possible diagnostics: (i) mass spectrometry for direct detection of clusters in the beam; (ii) monitoring of the flux as a function of  $P_0$  and  $T_0$ , showing the cluster formation by a change in the slope of the curves; (iii) measurement of the He time-of-flight distribution in the beam giving the velocity distribution, and therefore the stagnation temperature  $T_0$ ; (iv) LIF of a chromophore like Ca trapped on clusters giving a spectroscopic fingerprint of their presence; (v) detection of the fluorescence of a chemical reaction which is specific of the presence of clusters.

We used the last three diagnostics to get an evidence of the presence of He clusters in the beam.

### Speed distributions by He time-of-flight measurements ( $m=4$ )

Figure 4 displays different time-of-flight distributions for the mass 4 of He as a function of  $P_0$ , the stagnation temperature  $T_0$  being about 10 K. In these experiments, a 150 mm-diameter rotating chopper, with four slits of 0.5 mm width, is placed on the molecular beam path 800 mm after the optically probed zone. It selects bunches of particles with a 18.5 microseconds duration at half maximum: the time-of-flight of these neutral particles is measured between the chopper and the electron bombardment detector of the quadrupole mass filter located 2.275 m downstream. The length of the ionization zone is 5 mm and is negligible with respect to the flight length. The ion energy in the quadrupole mass filter is 10 eV, which means that the transit time for He<sup>+</sup> ions between the ion source and the channeltron is 13.5  $\mu$ s. This delay has to be subtracted from the experimental TOF.

On each spectrum, the number of He<sup>+</sup> ions is plotted as a function of their arrival time as well as the curve corresponding to the best fit by the theoretical time-of-flight distribution for helium monomers. Strictly speaking, the fit is only relevant for the TOF of monomers; when clusters are present, the fit is just indicative. The first spectrum on top of the figure is obtained for a stagnation pressure of 3.4 bars: it shows a single relatively wide peak related to helium monomers with a maximum at 7789  $\mu$ s and a FWHM of 310  $\mu$ s much larger than the chopper opening time, so that there is no need for a deconvolution by the chopper opening function; it corresponds to a flow speed  $U=292$  m/s and a Mach number of 45.8, i.e. a speed ratio  $S_{II}=Mach \times \sqrt{0.5 \times \gamma} = 41.8$  ( $\gamma=5/3$ ). From this time-of-flight distribution, it is possible to check the value of  $T_0$  by the enthalpy balance  $H_0 = \frac{1}{2} MU^2$  along a stream line of the flow, using the real helium gas enthalpy tabulated in Ref. [24]. On the middle panel of Fig. 4, at  $P_0 = 6.1$  bars, appears a second peak later and narrower which indicates the presence of clusters: the detected He<sup>+</sup> ions of this second peak are due to fragmentation of clusters upon electron bombardment, whereas the first peak still corresponds to ionized He monomers. The shift between the two peaks can be partly due to the velocity slip effect between heavy clusters and monomers during the expansion. The onset of this TOF cluster peak is in agreement with B.Schilling's thesis results [25]. On the bottom spectrum, at  $P_0 = 10.1$  bars, only the cluster peak remains with a very weak monomer signal. This peak corresponds to a flow speed  $U = 271$  m/s. The values of  $T_0$  range between 9.5 and 11.5 K as  $P_0$  varies between 6 and 25 bars. As  $P_0$  increases up to 72 bars,  $T_0$  rises up to 13.5 K: this is probably due to an increasing heat transfer to the cold parts of the source caused by the He background gas which has a pressure proportional to  $P_0$ . The average size of helium clusters is not measured in the experiment, but can be estimated from the stagnation conditions. For example, at  $P_0 = 20$  bars,  $T_0 = 11$  K, it ranges between  $1 \times 10^4$  and  $2 \times 10^4$  [16].

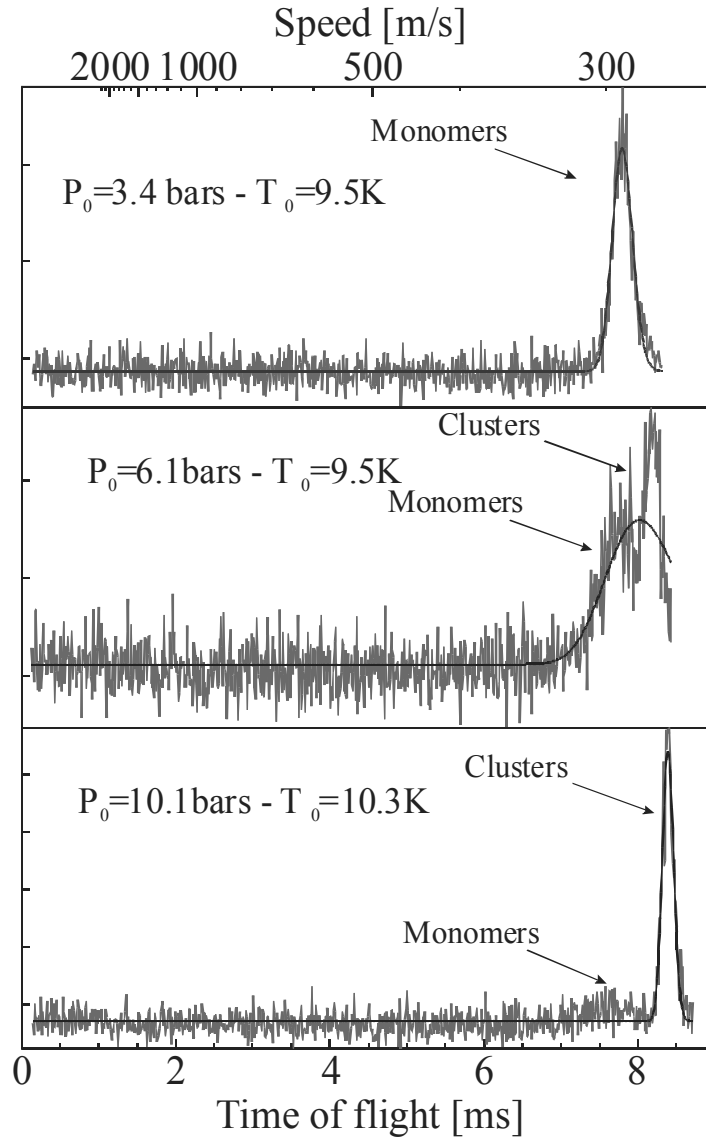


**FIGURE 4.** He time-of-flight distributions for different values of  $P_0$  and  $T_0$  around 10 K

### LIF of calcium trapped on helium clusters

We also performed Laser Induced Fluorescence experiments on a helium cluster beam passing through the calcium pick-up cell heated at 496 °C (Fig.1). The beam is extracted from a helium supersonic free jet formed with the stagnation conditions  $P_0 = 40$  bars,  $T_0 = 14.6$  K,  $D = 5$   $\mu\text{m}$ .

After laser excitation at a wavelength of 380 nm, far in the blue of the calcium resonance line and far from any allowed calcium transition, a fluorescence is observed on the resonance transition  $\text{Ca}(^1\text{P} \leftarrow ^1\text{S})$  of the free calcium at 422.7 nm (see Figure 5). This emission which could not occur in the gas phase is the evidence of He clusters, having captured one or several calcium atoms. Moreover the signal intensity vanishes when  $T_0$  increases above 20 K: this is also the evidence that He clusters are involved in the phenomenon. The LIF of calcium attached to He droplets has already been studied in the vicinity of the  $\text{Ca}(^1\text{P} \leftarrow ^1\text{S})$  at  $23652\text{cm}^{-1}$  resonance line by Stienkemeier et al. [26] suggesting an outside location of the Ca atom. Our results are obtained in very different conditions with a laser excitation at 380 nm ( $26316\text{cm}^{-1}$ ), far from any accessible level of Ca. This emission may be also due to excited calcium originating from the photodissociation of a Ca dimer that has been formed on the cluster by two successive pick-ups of calcium monomers [3, 11].

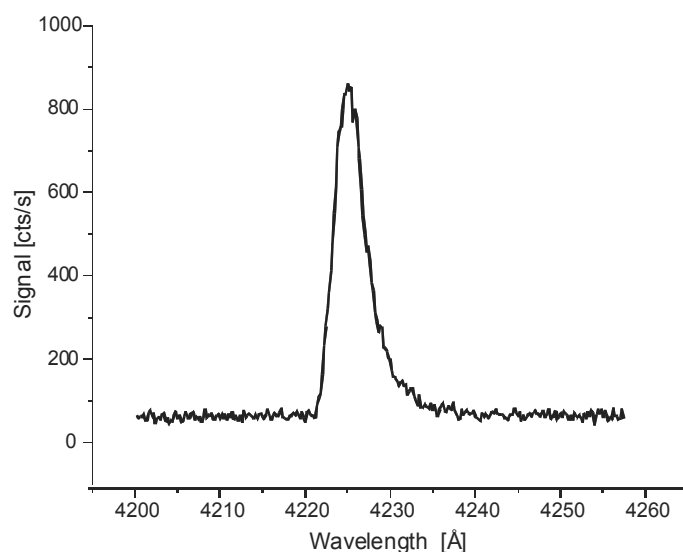


**FIGURE 5.** Dispersed LIF spectrum after excitation at 380 nm of calcium carried on He clusters. The emission corresponds to the Ca ( $^1P \leftarrow ^1S$ ) resonance line at 422.7 nm.

### The Ca+NO<sub>2</sub> system on (He)<sub>N</sub>

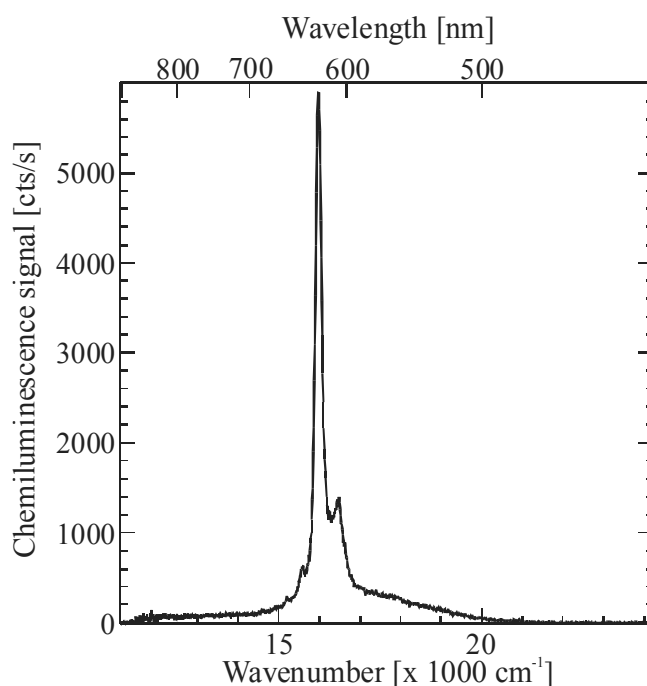


**FIGURE 6.** Chemiluminescence spectrum of CaO\* due the Ca...NO<sub>2</sub> reactive system trapped on He<sub>N</sub>

The reactive system Ca+NO<sub>2</sub> is not chemiluminescent in the gas phase as indicated in the literature [27] and verified in our experiment. However, with a double pick-up of calcium and NO<sub>2</sub> on a beam extracted from a helium free jet formed with stagnation conditions  $P_0 = 40$  bars,  $T_0 = 14.7$  K,  $D = 5\mu\text{m}$ , an intense fluorescence of CaO\* can be observed. The fluorescence spectrum extends from 480 to 870 nm, with a particularly strong component at 626 nm and two side bands at 606.5 and 641 nm corresponding to the « orange bands » [28] of CaO (Figure 6). This is an evidence of helium clusters of size sufficiently large to pick up several reactants (Ca and NO<sub>2</sub>) and change the reactive mechanism. As the reaction between one Ca atom and one NO<sub>2</sub> molecule is not exothermic enough ( $-0.944$  eV) to yield such a fluorescence, the observed reaction must involve a small aggregate (Ca<sub>n</sub> with  $n \geq 2$ ) and certainly several NO<sub>2</sub> (or N<sub>2</sub>O<sub>4</sub>) molecules in a concerted reactive process sufficiently exothermic.

## CONCLUSION

We have shown the possibility of modifying and operating our Campargue molecular beam source as a helium cluster beam source in non trivial experimental conditions and with a low pumping speed of about 1000 l/s. The accessible stagnation temperature ranges between 9.5 and 11.5 K for a stagnation pressure within 6 to 25 bars. As  $P_0$  increases up to 72 bars, the stagnation temperature rises up to 13.5 K.

Time-of-flight measurements of He at mass 4 allowed us to control the stagnation temperature  $T_0$  indicated by the sensors, and prove the presence of clusters for  $P_0$  above 6 bars at  $T_0 = 9.5$  K.

For  $T_0 = 14.6$  K and  $P_0 = 40$  bars, the helium cluster sizes are large enough to capture from one to several reactants as it is shown by the different experiments performed: the LIF of calcium captured upon  $\text{He}_N$  for an excitation wavelength of 380 nm, and the chemiluminescence of the excited CaO formed by the Ca+NO<sub>2</sub> reactive system trapped on helium clusters.

In the near future, we will continue our studies on the spectroscopy of calcium and calcium dimers, and also reactions involving Ca on  $\text{He}_N$ . In particular, we will try to find out what are the exact numbers of reactants Ca and NO<sub>2</sub> involved in the reactive process forming CaO\* from the Ca ... NO<sub>2</sub> system deposited on helium clusters.

## ACKNOWLEDGMENTS

The authors would like to thank M. Bougeard and Ph. Brédy for their technical help. They are grateful to L. Poisson, S. Soorkia and also the referees for their comments on the manuscript.

## REFERENCES

1. C. Gée, M. A. Gaveau, J. M. Mestdagh, M. A. Osborne, O. Sublemontier, and J. P. Visticot, *J. Phys. Chem.* **100**, 13421-13427 (1996).
2. J. M. Mestdagh, M. A. Gaveau, C. Gée, O. Sublemontier, and J. P. Visticot, *Int. Rev. Phys. Chem.* **16**, 215-247 (1997).
3. M. A. Gaveau, C. Gée, J. P. Visticot, and J. M. Mestdagh, *Comments At. Mol. Phys.* **34**, 241-258 (1999).
4. J. P. Visticot, P. de Pujo, J. M. Mestdagh, A. Lallement, J. Berlande, O. Sublemontier, P. Meynadier, and J. Cuvellier, *J. Chem. Phys.* **100**, 158-164 (1994).
5. B. Schilling, M. A. Gaveau, O. Sublemontier, J. M. Mestdagh, J. P. Visticot, X. Biquard, and J. Berlande, *J. Chem. Phys.* **101**, 5772-5780 (1994).
6. M. A. Gaveau, M. Briant, P. R. Fournier, J. M. Mestdagh, J. P. Visticot, F. Calvo, S. Baudrand, and F. Spiegelman, *Eur. Phys. J. D* **21**, 153-161 (2002).
7. M. A. Gaveau, M. Briant, P. R. Fournier, J. M. Mestdagh, and J. P. Visticot, *J. Chem. Phys.* **116**, 955-963 (2002).
8. A. Lallement, J. M. Mestdagh, P. Meynadier, P. de Pujo, O. Sublemontier, J. P. Visticot, J. Berlande, X. Biquard, J. Cuvellier, and C. G. Hickman, *J. Chem. Phys.* **99**, 8705-8712 (1993).
9. M. A. Gaveau, M. Briant, P. R. Fournier, J. M. Mestdagh, and J. P. Visticot, *Phys. Chem. Chem. Phys.* **2**, 831-837 (2000).
10. M. A. Gaveau, M. Briant, V. Vallet, J. M. Mestdagh, and J. P. Visticot, in *Atomic and Molecular Beams : The state of the Art 2000*, edited by R. Campargue, Berlin, Springer, 2001, pp. 827-838.
11. C. Gée, M. A. Gaveau, O. Sublemontier, J. M. Mestdagh, and J. P. Visticot, *J. Chem. Phys.* **107**, 4194-4206 (1997).
12. M. Briant, P. R. Fournier, M. A. Gaveau, J. M. Mestdagh, B. Soep, and J. P. Visticot, *J. Chem. Phys.* **117**, 5036-5047 (2002).
13. M. A. Gaveau, E. Gloaguen, P. R. Fournier, and J. M. Mestdagh, *J. Phys. Chem. A* **109**, 9494-9498 (2005).
14. J. A. Northby, *J. Chem. Phys.* **115**, 10065-10077 (2001).
15. J. P. Toennies and A. F. Vilesov, *Angew. Chem.-Int. Edit.* **43**, 2622-2648 (2004).
16. F. Stienkemeier and K. K. Lehmann, *J. Phys. B* **39**, R127-R166 (2006).
17. F. Stienkemeier and A. F. Vilesov, *J. Chem. Phys.* **115**, 10119-10137 (2001).
18. M. Hartmann, R. E. Miller, J. P. Toennies, and A. F. Vilesov, *Science* **272**, 1631-1634 (1996).
19. C. Callegari, K. K. Lehmann, R. Schmied, and G. Scoles, *J. Chem. Phys.* **115**, 10090-10110 (2001).
20. E. Lugovoj, J. P. Toennies, and A. Vilesov, *J. Chem. Phys.* **112**, 8217-8220 (2000).
21. R. Campargue, *J. Phys. Chem.* **88**, 4466-4474 (1984).
22. T. E. Gough, M. Mengel, P. A. Rowntree, and G. Scoles, *J. Chem. Phys.* **83**, 4958 (1985).
23. T.M. Flynn, "Cryogenic Fluids", in *Cryogenic Engineering*, New York, Marcel Dekker Inc., 1997, pp. 158-180.
24. R. D. Mc Carthy, *J. Phys. Chem. Ref. Data* **2**, 923 -1041 (1973).
25. B. Schilling, Ph. D.Thesis, Max-Planck-Institut für Strömungsforschung, Göttingen, 1993.
26. F. Stienkemeier, F. Meier, and H. O. Lutz, *J. Chem. Phys.* **107**, 10816-10818 (1997).
27. B. S. Cheong and J. M. Parson, *J. Chem. Phys.* **100**, 2637-2650 (1994).
28. C. S. Wei, S. W. Guo, and Y. P. Lee, *J. Chem. Phys.* **82**, 2942-2946 (1985).